JACS
JOURNAL OF THE AMERICAN CHEMICAL SOCIETY
Article
pubs.acs.org/JACS

Characterization of Streptonigrin Biosynthesis Reveals a Cryptic Carboxyl Methylation and an Unusual Oxidative Cleavage of a N−C Bond

Fei Xu,[†] Dekun Kong,[†] Xinyi He,[†] Zhang Zhang,[‡] Mo Han,[†] Xinqiang Xie,[†] Peng Wang,[†] Hairong Cheng,[†] Meifeng Tao,[†] Liping Zhang,[‡] Zixin Deng,[†] and Shuangjun Lin*[,†]

[†]State Key Laboratory of Microbial Metabolism, School of Life Sciences and Biotechnology, Shanghai Jiao Tong University, 800 Dongchuan Road, Shanghai 200240, China

[‡]College of Life Science, Hebei University, Baoding 071002, China

Supporting Information

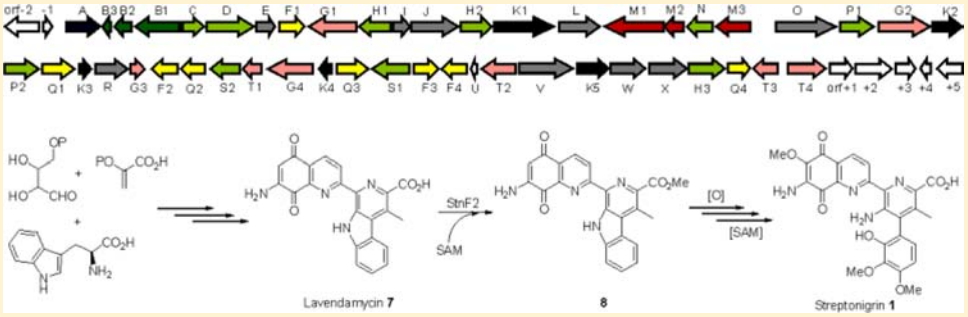

ABSTRACT: Streptonigrin (STN, **1**) is a highly functionalized aminoquinone alkaloid with broad and potent antitumor activity. Here, we reported the biosynthetic gene cluster of STN identified by genome scanning of a STN producer *Streptomyces flocculus* CGMCC4.1223. This cluster consists of 48 genes determined by a series of gene inactivations. On the basis of the structures of intermediates and shunt products accumulated from five specific gene inactivation mutants and feeding experiments, the biosynthetic pathway was proposed, and the sequence of tailoring steps was preliminarily determined. In this pathway, a cryptic methylation of lavendamycin was genetically and biochemically characterized to be catalyzed by a leucine carboxyl methyltransferase StnF2. A $[2Fe-2S]^{2+}$ cluster-containing aromatic ring dioxygenase StnB1/B2 system was biochemically characterized to catalyze a regiospecific cleavage of the N−C8′ bond of the indole ring of the methyl ester of lavendamycin. This work provides opportunities to illuminate the enzymology of novel reactions involved in this pathway and to create, using genetic and chemo-enzymatic methods, new streptonigrinoid analogues as potential therapeutic agents.

INTRODUCTION

Streptonigrin (STN, **1**) is an aminoquinone antitumor antibiotic produced by *Streptomyces flocculus* (ATCC13257).[1] STN was first reported in 1959,[1] and its molecular structure was initially established by chemical degradation and spectroscopic techniques in 1963.[2] Later, the accurate structure was confirmed by X-ray diffraction and ^{13}C NMR analysis in 1974−75.[3,4] The aminoquinolinone and pyridine rings of **1** are nearly coplanar, and the multisubstituted phenyl ring faces them perpendicularly.[4]

STN is active against a broad range of tumors, including breast, lung, head, and neck cancer, lymphomas and melanomas.[5−8] The antitumor mechanism studies have identified that **1** induces DNA single- and double-strand breaks, unscheduled DNA synthesis, DNA adduct formation, sister-chromatid exchanges, and chromosomal aberrations, inhibits topoisomerase II, and blocks synthesis of DNA and RNA.[9−11] In-depth investigations of the DNA damage mechanism revealed that **1** has shown multiple metal chelation effects and could bind to DNA irreversibly via STN−metal−DNA complexes.[12−15] In addition, **1** also shows in vivo and in vitro antiviral properties and potent, broad spectrum antibacterial activities against bacteria and fungi.[5,6]

The unique structure and potential in cancer therapy of **1** have attracted much attention from chemists and biologists. Great efforts have been made to chemically generate derivatives of **1** to improve its pharmaceutical properties.[16−22]

Biosynthetic studies in *S. flocculus* were performed using elaborate feeding experiments with isotopically labeled precursors by Gould and co-workers, suggesting that the aminoquinone moiety is derived from phosphoenolpyruvate and D-erythrose-4-phosphate via a shikimate-like pathway and L-tryptophan as another starting material provides β-methyltryptophan, a component forming the 4-phenylpicolinic acid moiety through an unknown cleavage of the indole ring.[23−31]

Received: July 16, 2012
Published: January 9, 2013

Subsequently, these two units form the core framework through an unknown condensation step with another molecule of D-erythrose-4-phosphate.[32] The isotope label experiments also established that the methyl groups including the C-methyl group originate from methionine.[26] Later, the methylation at the β-carbon of the tryptophan was biochemically confirmed to occur at an early stage of STN biosynthesis using a cell-free system in 1984.[33]

Nearly at the same period of time, lavendamycin and streptonigrone (**2**) were identified from *S. lavendulea* strain C22030 in 1981 and *Streptomyces* species IA-CAS isolate no. 114 in 1985, respectively.[34,35] Structurally, they and STN constitute a family of natural products called "streptonigrinoids" (Figure 1). From the view point of biosynthesis, whether there is a relationship between lavendamycin and STN has been put forward, but it is still unresolved.[17]

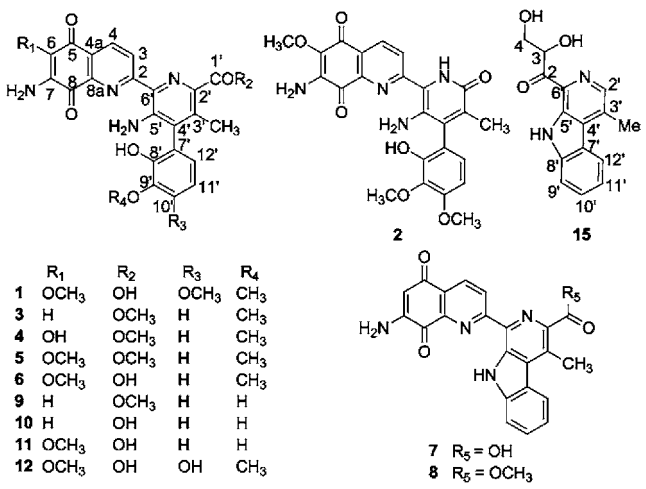

	R_1	R_2	R_3	R_4
1	OCH_3	OH	OCH_3	CH_3
3	H	OCH_3	H	CH_3
4	OH	OCH_3	H	CH_3
5	OCH_3	OCH_3	H	CH_3
6	OCH_3	OH	H	CH_3
9	H	OCH_3	H	H
10	H	OH	H	H
11	OCH_3	OH	H	H
12	OCH_3	OH	OH	CH_3

Figure 1. Structures of streptonigrin (STN, **1**) and related compounds.

Although numerous efforts have been made to decipher the biosynthetic pathway, the detailed biosynthetic mechanism of **1** still remains unclear. In order to identify the biosynthetic steps, we cloned and sequenced the biosynthetic gene cluster of **1**. In this paper, we describe the cluster consisting of 48 genes putatively responsible for biosynthesis of **1** and the proposal of its biosynthetic pathway containing a cryptic methylation. Lavendamycin (**7**) was proved to be the pivotal intermediate for STN biosynthesis. StnB1 and StnB2 were biochemically characterized to be responsible for the cleavage of the N−C bond of the methyl ester of **7** to initiate modification steps, the orders of which were preliminarily determined by identification of the structures and feeding experiments of the compounds accumulated by specific gene inactivation mutants of the producing strain.

RESULTS AND DISCUSSION

Identification and Verification of the Biosynthetic Gene Gluster of STN in *S. flocculus* CGMCC 4.1223. The genome sequencing of *S. flocculus* CGMCC 4.1223, a producer of **1**, yielded a 7.1 Mb DNA sequence and identified a likely homologue of the C-methyltransferase MppJ that catalyzes β-methylation of phenylalanine in mannopeptimycin biosynthesis.[36] A similar reaction has been confirmed to be involved in transformation of tryptophan to β-methyltryptophan, which is the proposed first step of STN biosynthesis.[28,33] This homologue led to identification of the putative gene cluster of **1** that was localized on a contiguous ~65 kb DNA region (NCBI database accession number JQ414024). Bioinformatics analysis revealed 55 open reading frames (orfs) within this region (Figure 2 and Table S1, Supporting Information). We constructed a genomic library in *Escherichia coli* using the cosmid vector pJTU2554, and three overlapped cosmids (p4D6, p4F4, and p3A8) were identified to cover this DNA region.[37] To verify the involvement of this DNA region in the biosynthesis of **1**, we constructed a large fragment deletion mutant (see the Supporting Information). As expected, the resulting mutant completely abolished **1** production, confirming its involvement in **1** biosynthesis (Figure S1, Supporting Information).

Determination of Boundaries of the *stn* Gene Cluster. To determine the boundaries of the gene cluster, a series of polymerase chain reaction (PCR)-targeting gene replacement

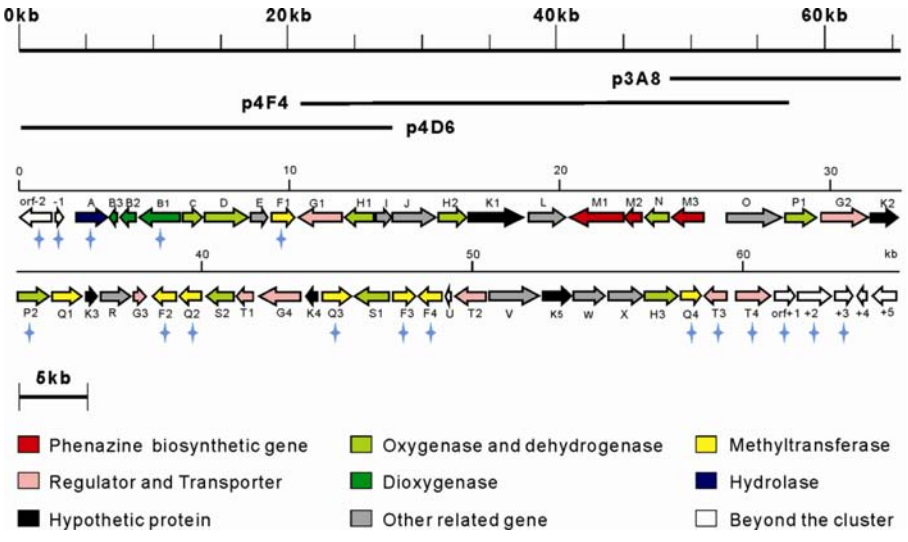

Figure 2. Map of the streptonigrin biosynthetic gene cluster in *S. flocculus* CGMCC4.1223. Genes are color-coded according to their putative functions (the orfs labeled with blue star symbols were inactivated in this study).

dx.doi.org/10.1021/ja3069243 | J. Am. Chem. Soc. 2013, 135, 1739−1748

experiments were performed. The two genes *orf-1* and *orf-2* located upstream of the 65 kb DNA region were predicted to encode a prolyl-tRNA synthetase and a DNA binding protein, respectively. These two genes were predicted not to be related to **1** biosynthesis. Indeed, inactivation of both genes with the replacement of the *aac(3)IV* gene did not show any influence on **1** production (Figure S1, Supporting Information, and Figure 3A, trace ii). In contrast, inactivation of *stnA* encoding

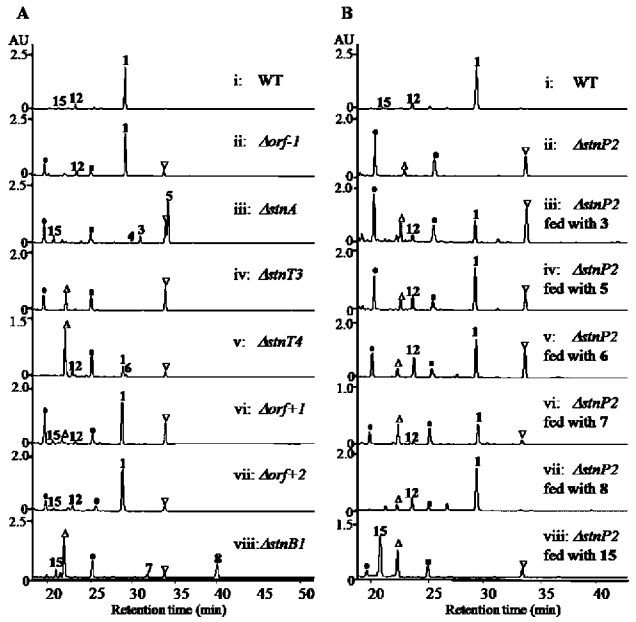

Figure 3. HPLC profiles of fermentation extracts of *S. flocculus* CGMCC4.1223 wild-type (i) and mutant strains (ii–viii) with detection at 245 nm. The compounds (Δ), (■), (●), and (▽) were determined not to be related to STN. The Arabic numbers indicate the compounds in Figure 1.

an α/β-fold hydrolase completely abolished **1** production but accumulated three new compounds (**3**, **4**, and **5**) as judged by high-performance liquid chromatography (HPLC) analysis (Figure 3A, trace iii). Therefore, the left boundary of this gene cluster was determined at *stnA*.

To locate the right boundary of the gene cluster, five adjacent genes from *stnT3* to *orf+3* were inactivated by the insertion of the *aac(3)IV* gene, respectively. Inactivation of *stnT3* encoding a LuxR family transcriptional regulator completely abolished **1** production (Figure 3A, trace iv). *stnT4* encodes a protein resembling a cyanate transporter, a member of the major facilitator superfamily (MFS) transporters.[38] HPLC analysis of the fermentation extract of the Δ*stnT4* mutant revealed significantly reduced production of **1** and accumulation of trace amounts of **6** (Figure 3A, trace v). The adjacent genes *orf+1* to *orf+3* encode proteins homologous to ArsR family transcriptional regulator, monooxygenase, and methyltransferase, respectively. Individual inactivation of *orf+1* to *orf+3* did not affect the production of **1** (Figure S1, Supporting Information, and Figure 3A, traces vi and vii). *stnT4* was determined to be the right boundary of the *stn* gene cluster. Thus, we proposed that 48 genes (*stnA–T4*) are probably involved in STN biosynthesis as shown in Figure 2 and Table S1 of the Supporting Information.

Compounds **3** and **5** were purified from the fermentation extracts of the Δ*stnA* mutant for structural characterization. Compound **5** (22.4 mg) was obtained and used to complete NMR experiments. The signals [δ_H 7.08 (d, J = 7.5 Hz, 1H), 6.96 (t, J = 7.5 Hz, 1H), 6.63 (d, J = 7.5 Hz, 1H)] indicated that **5** contains an adjacent trisubstituted phenyl ring (Figure S4 and Table S2, Supporting Information). The full NMR analysis including ^{13}C NMR, ^{1}H–^{1}H COSY, HSQC, and HMBC, along with high-resolution mass spectrometry (HR-MS) analysis (m/z: obsd. 491.1589, calcd. 491.1561 for $[C_{25}H_{23}N_4O_7]^+$), identified **5** as a methyl ester of 10′-desmethoxystreptonigrin (Figures S5–8 and Tables S3 and S4, Supporting Information).[39] For compound **3**, the observed exact mass 461.1485 (calcd. 461.1456 for $[C_{24}H_{21}N_4O_6]^+$), 30 Da less than that of **5**, indicated that **3** has one fewer methoxyl group than **5**. The ^{1}H NMR spectrum showed the methoxyl proton signal at δ_H 3.82 (s, 3H) in **5** was absent in **3**, while a methine proton signal appeared at δ_H 5.87 (s, 1H) in **3** (Figure S9 and Table S2, Supporting Information). The ^{13}C NMR spectrum showed that, apart from the loss of a methoxyl carbon at δ_C 59.7, the chemical shifts of C-6 and C-7 were shifted from 135.7 and 141.5 to 101.6 and 150.7, respectively, which were consistent with those measured for the aminoquinone part of lavendamycin (Figure S10 and Table S3, Supporting Information).[34] Thereby, **3** was identified as the 6-desmethoxylation product of **5**, as shown in Figure 1. The time course of the production of **3** and **5** in the Δ*stnA* mutant strain showed that **3** was converted to **5** with **4** as a putative intermediate (Figure S2, Supporting Information). The rapid conversion of **4** to **5** hindered the purification of **4** for NMR analysis. Compound **4** was proposed to be the 6-hydroxylated version of **3** based on HR-MS/MS analysis (obsd. 477.1400, calcd. 477.1405 for $[C_{24}H_{21}N_4O_7]^+$) compared with that of **5** (Figure S11, Supporting Information).

Large-scale fermentation of Δ*stnT4* was carried out to provide sufficient amounts of **6** for its structural elucidation. HR-MS analysis (obsd. 477.1412, calcd. 477.1405 for $[C_{24}H_{21}N_4O_7]^+$), along with the ^{1}H NMR spectrum (Figure S12, Supporting Information) confirmed **6** to be 10′-desmethoxystreptonigrin.[39] Structurally, **6** was supposed to be an intermediate for **1** biosynthesis, indicating that hydroxylation and subsequent methylation at position-10′ should be the last two steps of **1** biosynthesis. The reason why the inactivation of *stnT4* down-regulated **1** production and accumulated **6**, needs to be further investigated.

Feeding the Nonproducing Mutant Δ*stnP2* with Compounds 3, 5, and 6. Compounds **3** and **5** were identified to be methyl esters, while **1** is a free carboxylic acid. As a result, one would ask whether these compounds are intermediates or shunt products of the STN biosynthetic pathway. To solve this issue, we would carry out feeding experiments with **3** and **5**, so we had to construct a mutant that blocks the biosynthesis of **1** at an early stage. *stnP2* encodes an FAD-dependent oxidoreductase that shows high sequence homology to D-amino acid oxidase (37/52, identity/similarity).[40,41] We propose that StnP2 may participate in the β-methylation of tryptophan by catalyzing the oxidative deamination of amino acids to keto acids. This β-methylation is the proposed first step of the biosynthetic pathway of STN described by Gould and Darling.[28] As expected, inactivation of *stnP2* completely abolished production of **1**, without production of new metabolites related to STN biosynthesis (Figure 3B, trace ii). Therefore, the Δ*stnP2* mutant strain was used as the host to carry out the feeding experiments with **3** (1 mg) and **5** (2.5 mg). HPLC analysis profiles displayed that both

dx.doi.org/10.1021/ja3069243 | J. Am. Chem. Soc. 2013, 135, 1739–1748

were completely converted to **1** (Figure 3B, traces iii and iv), suggesting that **3**−**5** are biosynthetic intermediates of **1**.

The above results provided valuable information on STN biosynthesis: (i) methylation at position-9′ precedes the modifications at position-6 and position-10′; (ii) subsequently, hydroxylation followed by methylation at position-6 occurs; (iii) hydroxylation and subsequent methylation at position-10′ are the last two steps of STN biosynthesis; (iv) methyl esterification of the carboxylate at position-1′ may occur prior to the modification of position-9′. Apparently, this step reaction is cryptic in the STN biosynthesis. Several cryptic reactions involved in biosynthesis of secondary metabolites have been reported recently. Cryptic chlorination catalyzed by nonheme and α-ketoglutarate-dependent halogenases initiated cyclopropane ring formation in biosynthesis of coronitine,[42] kutzneride,[43] and curacin A.[44] The cryptic acylation of the N-terminus was adopted as an activation strategy in nonribosomal peptide synthesis of saframycin A, didemnin B, and xenocoumacin.[45−47] The biosynthesis of caerulomycin was also proposed to involve an extra cycle of elongation with leucine catalyzed by a non-ribosomal pepetide synthetase CrmB.[48] The same cryptic methyl esterification strategy has also been used in the biosynthesis of the antibiotics capuramycin and thiostrepton as well as the primary metabolite biotin.[49−51] The methyl esterification in the biosynthesis of capuramycin aimed to activate the carboxyl group to facilitate amide bond formation,[49] while the methyl esters were hydrolyzed by catalysis of α/β-fold hydrolases to release the free carboxylic acid intermediates during maturation of thiostrepton and biotin.[50,51] Although StnA shows no significant sequence homology to reported α/β-fold hydrolases, it displays the characteristics of α/β-fold hydrolases,[52] so StnA is proposed to be an esterase hydrolyzing the methyl ester at position-1′ of **5** to provide **6**, the substrate for the hydroxylation and methylation at the position-10′. Therefore, we carried out a further feeding experiment with **6** into the Δ*stnP2* mutant strain. Compound **6** was also completely incorporated into **1** (Figure 3B, trace v), supporting the assignment of StnA and **3**−**6** as the biosynthetic intermediates of **1**.

Inactivation of *stnB1* Putatively Involved in the Cleavage of the N−C Bond. The identification of intermediates **3**−**6** allowed us to reason that **1** is maturated via several sequential tailoring modifications from a certain pivotal intermediate. The previous feeding study with ^{15}N- and ^{13}C-labeled tryptophan combining use of ^{15}N−^{13}C couplings in ^{13}C NMR spectroscopy suggested that **1** was biosynthesized via an unusual oxidative cleavage of the N−C8′ bond of a β-carboline alkaloid-like intermediate catalyzed by a kind of oxidative enzyme.[27] The *stnB1*−*B3* genes encode proteins resembling aromatic ring dioxygenase α and β subunits and ferredoxin, respectively. Similar enzymes systems act on phenyl groups to form diols as the first step in the oxidative degradation of aromatic compounds.[53,54] We proposed that StnB1−3 may be involved in the cleavage of the N−C bond. To probe this hypothesis, we constructed the replacement mutant of *stnB1*, a main component in this enzyme system, by *aac(3)IV* using the PCR-targeting method (see the Supporting Information). As expected, deletion of *stnB1* completely abolished production of **1**, resulting in accumulation of new compounds **7** and **8** (Figure 3A, trace viii). Compound **15** was also found to be produced in an increased amount, compared to the wild type.

To determine their structures, **7**, **8**, and **15** were purified from the fermentation extracts of the Δ*stnB1* mutant. HR-MS analysis of **7** gave the ion peak at *m*/*z* 399.1095 (calcd. 399.1088, for $[C_{22}H_{15}N_4O_4]^+$). Strikingly, both mass and UV−visible absorption profiles of **7** were reminiscent of lavendamycin (Figure S3, Supporting Information).[55] This prompted us to purify sufficient **7** (0.8 mg) for NMR analysis. ^{1}H NMR data consistent with those reported confirmed **7** to be lavendamycin (Figure S13 and Table S2, Supporting Information).[34,55] The molecular formula of **8** was determined to be $C_{23}H_{16}N_4O_4$ by HR-MS (obsd. 413.1252, calcd. 413.1244 for $[M + H]^+$), which is an increase of 14 Da compared to that of **7** suggesting that it is a methylated version of **7**. Compared to the ^{1}H NMR data reported,[34] **8** was identified as a methyl ester of **7** (Figure S14 and Table S2, Supporting Information).[56] HR-MS analysis (obsd. 271.1078, calcd. 271.1077 for $[C_{15}H_{15}N_2O_3]^+$), along with one-dimensional (1D) and two-dimensional (2D) NMR analyses of **15**, identified it as oxapropaline D, which was previously identified from the producer of lavendamycin (Figures S15 and S16, Supporting Information).[55]

Feeding the Nonproducing Mutant Δ*stnP2* with Compounds 7, 8, and 15. Lavendamycin was identified from Δ*stnB1*, which provides a chance to test whether lavendamycin is an intermediate or shunt metabolite of the biosynthetic pathway of **1**.[17] Thereupon, we fed **7** (0.6 mg) and **8** (2 mg) to Δ*stnP2*, separately (see the Supporting Information). LC-MS analyses of the fermentation extracts confirmed that **1** production was indeed restored in both cases (Figure 3B, traces vi and vii). The complete conversion of **7** and **8** into **1** suggested that both may serve as efficient precursors for STN biosynthesis. However, the feeding **15** (1.5 mg) into Δ*stnP2* did not restore the production of **1**, suggesting that **15** is likely to be a shunt product of the biosynthetic pathway of **1** (Figure 3B, trace viii).

The production level of **7** is about 20-fold lower than that of **8** in Δ*stnB1*, and both were efficiently fed into the nonproducing Δ*stnP2* mutant to chemically rescue the production of **1**. These data supported an assumption that the cryptic methylation of a carboxylate probably occurred on **7**. The methyl ester of STN was reported less toxic and to have a higher therapeutic index than the parent acid.[57,58] The possible motivation of the methyl ester formation could be attributed to decreasing the cytotoxicity of the descendent STN analogues to protect the host.

Characterization of the Cleavage of the N−C8′ Bond Catalyzed by StnB1/B2. StnB1−B3 belong to the Rieske-type dioxygenase system that also includes a ferridoxin reductase, examplified by the degradation enzymes of benzofuran and carbozole (Figure S17, Supporting Information).[59,60] Thereby, we proposed that StnB1−B3 may be involved in catalyzing the cleavage of the N−C8′ bond of **8** by an oxidative process (Figure 4A). To gain biochemical evidence, StnB1 and B2 were overexpressed in *E. coli* BL21 (DE3) as N-terminal His_6-tagged fusion proteins and purified to near homogeneity (Figure S18, Supporting Information). Sequence alignment revealed StnB1 to be a $[2Fe−2S]^{2+}$-dependent dioxygenase α subunit, so active StnB1 was reconstituted with $Fe(NH_4)_2(SO_4)_2$ and Na_2S in the presence of dithiothreitol. In an in vitro assay, the reconstituted StnB1 and dioxygenase β subunit StnB2 were incubated with 0.1 mM $Fe(NH_4)_2(SO_4)_2$, 0.1 mM **8**, and 1 mM sodium dithionite ($Na_2S_2O_4$) as a source of electrons instead of ferridoxin

dx.doi.org/10.1021/ja3069243 | J. Am. Chem. Soc. 2013, 135, 1739−1748

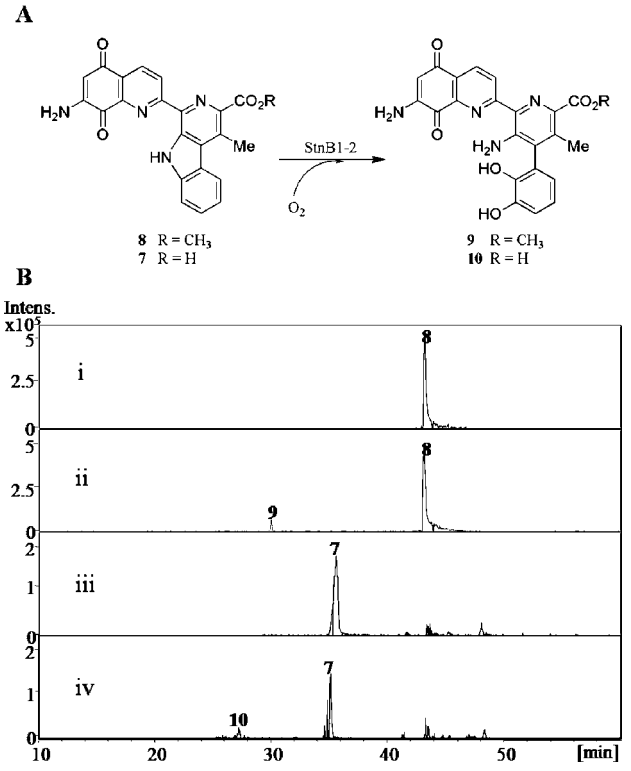

Figure 4. Biochemical characterization of StnB1/B2-catalyzing dioxygenation of **7** and **8** in vitro. (A) Reaction catalyzed by StnB1/B2. (B) LC-extracted ion chromatography MS (EIC-MS) of the reactions for 4h: (i) boiled StnB1/B2 with **8**; (ii) reconstituted StnB1/B2 with **8**; (iii) boiled StnB1/B2 with **7**; (iv) reconstituted StnB1/B2 with **7**.

(StnB3) and ferridoxin reductase, required for reduction of the $[2Fe-2S]^{2+}$ cluster in 50 mM MES buffer containing 5% DMSO to improve solubility of **8**. As expected, a new peak was detected by LC-HR-MS analysis (Figure 4B, trace ii), which gave an $[M + H]^+$ ion at m/z 447.1299 (calcd. 447.1299 for $[C_{23}H_{19}N_4O_6]^+$). Compared to that of **3**, tandom MS analysis suggested the structure of the product as **9** (Figure S19, Supporting Information). To the contrary, this product was not detected in the control reaction that was carried out with boiled StnB1/B2 in the same condition (Figure 4B, trace i). Moreover, we also tested the activity of the StnB1/B2 using **7** as a surrogate. The similar ring-opening product **10** was detected by LC-HR-MS analysis (Figure 4B, trace iv and Figure S19, Supporting Information), while the time course of the StnB1/B2-catalyzing reaction with **7** and **8** as cosubstrates showed that the cleavage of **8** seemed to be faster than that of **7**, especially in the first hour (Figure S20, Supporting Information). Along with the identified intermediates **3**−**5**, which bear a methyl group at position-1′ as esters, these results suggested that the StnB1/B2 system most probably catalyzed the regiospecific cleavage of the N−C8′ bond of **8** to form an amino group at C5′ and two hydroxyl groups at C8′ and C9′, the proposed substrate of the biosynthesis of **3**.

Characterization of Methyl Esterification of Lavendamycin in Vivo and in Vitro. Together with the production of **7** and **8** in the Δ*stnB1* mutant and feeding experiments, the biochemical characterizations of StnB1/B2 support the hypothesis that **7** is the substrate of the methyl esterification. In search for the candidate catalyzing this methyl esterification, we paid attention to the genes *stnF1*−*4* that encode four leucine carboxyl methyltransferases (LCM superfamily) with high homology to each other (Figure S21, Supporting Information). The LCM-like methyltransferases usually modulate eukaryotic proteins by methylating C-terminal carboxyl groups.[61,62] To evaluate whether they are related to the STN biosynthesis and which may catalyze this methyl esterification, we constructed their gene replacement mutants using PCR-targeting technology, respectively. LC-MS was employed to analyze the fermentation extracts of all mutant strains. The Δ*stnF1* and Δ*stnF2* mutants produced trace or reduced amounts of **1** (Figure 5A, traces ii and iii). However, both

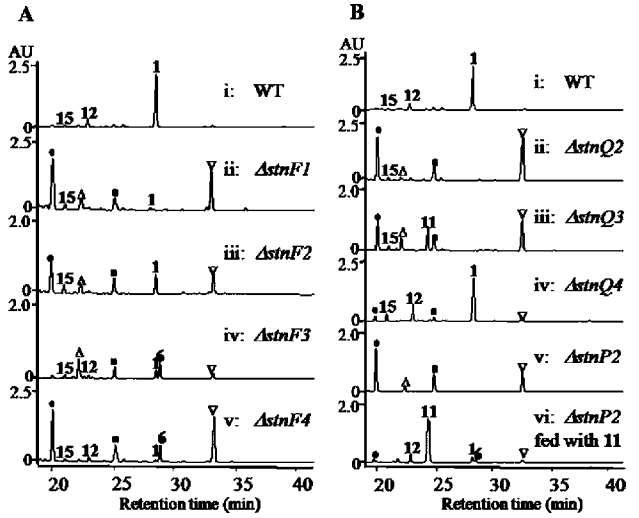

Figure 5. HPLC profiles of fermentation extracts of *S. flocculus* CGMCC4.1223 wild-type (i) and mutant strains (ii−vi) with detection at 245 nm. The compounds (Δ), (■), (●), and (▽) were determined not to be related to STN. The Arabic numbers indicate the compounds in Figure 1.

Δ*stnF3* and Δ*stnF4* mutants produced small or trace amounts of **1** and larger amounts of compound **6** (Figure 5A, traces iv and v). These results confirmed the involvement of these four genes in the biosynthesis of **1**. As demonstrated above, the StnB1/B2 system can recognize both acid form **7** and ester form **8** to catalyze the oxidative cleavage of the N−C8′ bond, so we can speculate that StnF1 or StnF2 may catalyze the methyl esterification of **7** to generate **8**. However, StnF3 and StnF4 are not appropriate candidates for this methylation because of accumulation of the intermediate **6** in their inactivation mutants. They may either modulate the enzymes acting at the last two steps so that their inactivation accumulated **6**, or play other roles in the biosynthesis of **1**, which remains unclear.

To determine whether StnF1 or StnF2 catalyzes the methyl esterification of **7**, we overexpressed StnF1 and StnF2 in *E. coli* BL21 (DE3) as N-terminal His_6-tagged fusion proteins and purified them to near homogeneity (Figure S22A,B, Supporting Information). In the presence of SAM, StnF2 can efficiently catalyze the methylation of **7** to generate **8**, but StnF1 cannot (Figure S22C, Supporting Information). The controls were carried out with boiled enzymes in the same condition (Figure S22C, Supporting Information). These results not only confirmed that the cryptic methylation occurred on **7** but also determined that **8** is the native substrate of the StnB1/B2 system. Lavendamycin **7** was not detected from the Δ*stnF2* mutant, even though the fermentation was monitored at

dx.doi.org/10.1021/ja3069243 | J. Am. Chem. Soc. 2013, 135, 1739−1748

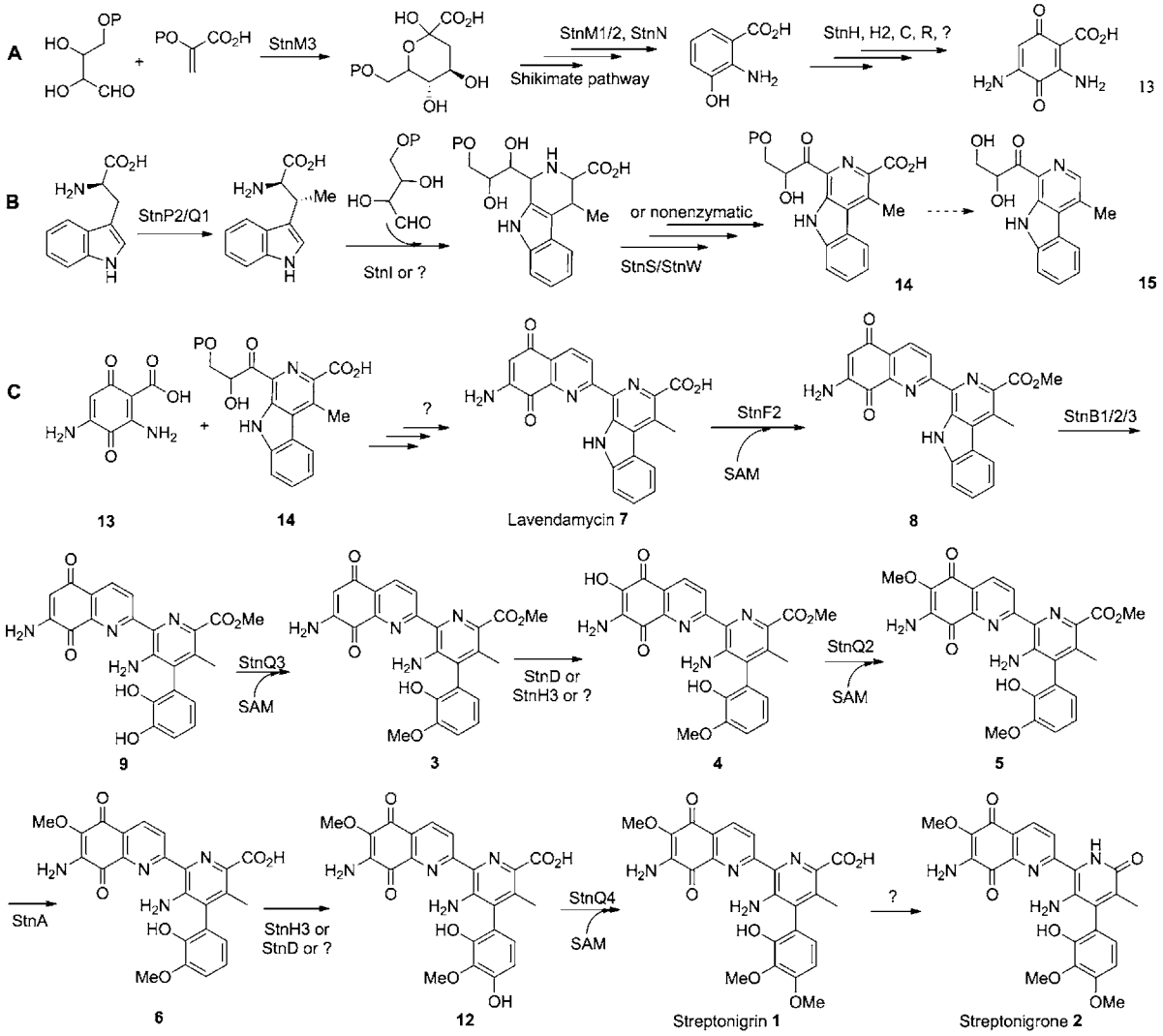

Figure 6. Proposed biosynthetic pathway of streptonigrin. (A) Proposed biosynthetic pathway of the putative intermediate **13**. (B) Proposed biosynthetic pathway of the putative intermediate **14**. (C) Proposed lavendamycin formation and following hydroxylation, methylation steps supported by isolated intermediates (**3**, **4**, **5**, **6**, **7**, **8**, and **12**), and shunt product (**15**) from Δ*stnA*, Δ*stnB1*, Δ*stnQ4*, and Δ*stnT4* mutants and feeding experiments.

different fermentation time points (3 days, 4 days, until 7 days), indicating that the StnB1/B2 system is less specific toward the acid and ester forms of lavendamycin, consistent with the results of the biochemical characterizations of StnB1/B2. Compound **1** is still produced in this mutant, albeit in the reduced level, implying that the oxidases and methyltransferases for the post modifications have flexible substrate specificities.

Inactivation of Genes Encoding O-Methyltransferase. The *stn* cluster contains three genes (*stnQ2*, *stnQ3*, and *stnQ4*) encoding SAM-dependent O-methyltransferase. They were proposed to catalyze methylations of the hydroxyl groups at position-6, -9′, and -10′. To determine the timing of the methylation catalyzed by each methyltransferase, inactivation of each gene was performed by the insertion of the *aac(3)IV* gene (see the Supporting Information). *stnQ2* encodes a methyltransferase showing high sequence homology to the catechol O-methyltansferase (identity 64% and similarity 79%).[63] It was proposed to catalyze the methylation at position-6 (pseudocatechol) or postion-9′ (catechol, Figure 6C). Unexpectedly, the Δ*stnQ2* mutant totally abolished **1** production, and other HPLC peaks were characterized to be unrelated to STN (Figure 5B, trace ii). StnQ3 has 26% identity and 46% similarity to AziB2 involved in antitumor antibiotic azinomycin B biosynthesis.[64,65] The Δ*stnQ3* mutant did not produce **1** but accumulated a new compound, **11** (Figure 5B, trace iii). StnQ4 shows low homology to ubiquinone/menaquinone biosynthesis methyltransferase. The Δ*stnQ4* mutant still produced comparative amounts of **1**, along with higher amounts of **12** than the wild-type strain (Figure 5B, trace iv).

Large-scale fermentation of both Δ*stnQ3* and Δ*stnQ4* mutants supplied sufficient samples for the characterization of their structures. HR-MS analysis of **11** showed the ion peak at *m*/*z* 463.1290, suggesting the molecular formula $C_{23}H_{18}N_4O_7$ (calcd. 463.1248, for $[C_{23}H_{19}N_4O_7]^+$). 1D and 2D NMR analyses identified **11** as 9′-desmethylated version of **6** (Figures S23−27, Supporting Information). This may support the assignment of StnQ3 responsible for the methylation at position-9′ of **9**, the product of StnB1/B2 (Figure 5C). HR-MS analysis of **12** revealed the ion peak at *m*/*z* 493.1386 (calcd. 493.1354 for $[C_{24}H_{21}N_4O_8]^+$), consistent with that of the 10′-desmethylated version of **1**. The ^{1}H NMR spectrum (Figure S28, Supporting Information) confirmed its identity.[66] The

dx.doi.org/10.1021/ja3069243 | J. Am. Chem. Soc. 2013, 135, 1739−1748

increased production of **12** from Δ*stnQ4* suggested that StnQ4 may be responsible for this last methylation step (Figure 6C), while the production of **1** might be due to the complementation of other unknown methyltransferases in the genome that contains 18 similar methyltransferase-encoding genes. These data allow us to propose that StnQ2 may catalyze the methylation of the hydroxyl at C6 (Figure 6C). Its deletion mutant did not accumulate the anticipated intermediate probably due to polar effect.

Feeding the Nonproducing Mutant Δ*stnP2* with Compound 11. Compounds **3**−**5** bearing the methyl group at position-9′ and their production sequence strongly suggested methylation at position-9′ prior to that at position-6. However, **11** has only one methoxyl group at position-6 not position-9′. To define the order of O-methylation at position-6 and -9′ in the biosynthesis of **1**, we fed **11** (2 mg) to the nonproducing Δ*stnP2* mutant (Figure 5B, trace vi). About 5% of **11** was observed to be incorporated into **1**, while **3** and **5** can perfectly restore **1** production in Δ*stnP2*, suggesting that **11** is a putative shunt metabolite of the biosynthetic pathway of **1** and the methylation at position-9′ indeed occurs prior to that at position-6. These results indicated that the tailoring enzymes, to some degree, have flexible substrate specificity, analogous to methyltransferases in spinosyn biosynthesis.[67] Thus, we can propose the sequence of the methylations: StnQ3 catalyzes the first methylation at position-9′, StnQ2 may catalyze the second at position-6, and StnQ4 is probably for the last at position-10′ (Figure 6C).

On the basis of our current genetic, chemical, and biochemical data, along with bioinformatics analysis, we can propose a putative biosynthetic pathway for STN shown in Figure 6. The first building block, 3-hydroxyanthranilic acid, was biosynthesized from D-erythrose-4-phosphate and phosphoenol pyruvate via a branch of the shikimate pathway catalyzed by StnM1−M3 and StnN (Figure 6A).[68−70] *stnM1*−*M3* genes encode the homologues of the enzymes involved in the phenazine biosynthesis including a 3-deoxy-D-arabinoheptulosonate 7-phosphate (DAHP) synthase (StnM3), a 2-amino-deoxyisochorismate (ADIC) synthase (StnM1),[71] and an isochorismatase (StnM2). *stnN* encodes a 2,3-dihydroxybenzoate-2,3-dehydrogenase involved in the biosynthesis of 2,3-dihydroxybenzoic acid, a precursor for biosynthesis of some siderophores.[72,73] Next, the 6-hydroxylation of 3-hydroxyanthranilic acid was probably catalyzed by StnH2, a predicted FAD-dependent salicylate hydroxylase. The subsequent formation of aminoquinone may involve NADPH: quinone reductases StnC or StnH1 catalyzing dehydrogenation and StnR, a sole pyridoxal phosphate (PLP)-dependent aminotransferase putatively responsible for the incorporation of amino group at C7 to provide the key intermediate **13** (Figure 6A).

On the other hand, C-methylation of tryptophan yields *β*-methyltryptophan probably catalyzed by the combination of D-amino acid oxidase StnP2 and C-methyltransferase StnQ1. Next, the *β*-methyltryptophan condenses with D-erythrose-4-phosphate via a pictet-spengler reaction probably catalyzed by StnI (cyclase/dehydrase),[45] followed by dehydrogenation that is catalyzed by dehydrogenases/oxidoreductases such as StnS1 (cytochrome P450) and StnW (acyl−CoA dehydrogenase), or spontaneous to produce *β*-carboline intermediate **14** (Figure 6B). The proposal of **14** as the intermediate for **1** biosynthesis can be supported by the production of **15** in the wild type and most mutants except Δ*stnP2*, Δ*stnT3*, and Δ*stnT4*. Compound **15** is supposed to be the product of an unscheduled decarboxylation and hydrolysis of **14**.

The intermediate **13** reacts with **14** via an unknown process to form lavendamycin **7** (Figure 6C). Subsequently, the methyl esterification of **7** yields **8**, catalyzed by StnF2. After the StnB1−3 system catalyzes the cleavage of the N−C8′ bond of **8** to provide **9**, StnQ3 catalyzes the first O-methylation to give **3**. The hydroxylation of **3** at position-6 is probably catalyzed by StnD, a predicted two-component FAD-dependent 4-hydroxyphenylacetate-3-hydroxylase or StnH3, a putative FAD-binding oxidoreductase, or another oxidoreductase to produce **4** that is methylated by StnQ2 to form **5**. StnA catalyzes the hydrolysis of **5** to generate **6** that undergoes a hydroxylation at position-10′ mediated by StnD or StnH3, or other oxidoreductase, and a methylation putatively catalyzed by StnQ4, to form the final product **1**. Furthermore, **1** undergoes a decarboxylation and oxidation to generate **2**, a member of the streptonigrinoid family and a minor component reported in STN-producing strain.[35]

■ CONCLUSION

In summary, we identified the biosynthetic gene cluster of STN in *S. flocculus* CGMCC4.1223 by genome scanning and targeted gene disruption. We generated 17 gene inactivation mutants, from five of which we identified nine compounds. On the basis of the structures of the accumulated compounds, the feeding studies, biochemical characterizations, and bioinformatics analysis of each gene, we proposed the putative biosynthetic pathway of STN that contain a cryptic methylation of a carboxylate. Lavendamycins (**7** and **8**) were proved to be pivotal precursors of STN biosynthesis by feeding them into the nonproducing Δ*stnP2* fermentation medium to rescue STN production in Δ*stnP2* and biochemical characterizations. The StnB1/B2 system was preliminarily characterized to catalyze the regiospecific cleavage of the N−C8′ bond of the indole ring in **8**. Our findings pave the way for studying of the enzymology of novel reactions involved in STN biosynthesis and exploration of the potential of combinatorial biosynthesis for the generation of STN derivatives for clinical use as cancer therapy.

■ EXPERIMENTAL SECTION

Bacterial Strains, Plasmids, and Reagents. The bacterial strains and plasmids used in this study are listed in Table S4 of the Supporting Information, and the primers used in this study are listed in Table S5 of the Supporting Information. Primers were synthesized in Sangong Biotech Co. Ltd. Company (Shanghai, China). All DNA sequencing was performed in DNA Bio Tech Co. Ltd. (Shanghai) and Major Biotech Co. Ltd. (Shanghai). Chemical reagents were purchased from Lingfeng (Shanghai) Co. Ltd. Restriction enzymes were purchased from New England Biolabs (Ipswich, MA) and Fermentas (St. Leon-Rot, Germany). Taq DNA polymerase and DNA ligase were purchased from Takara Co. Ltd. Company (Dalian, China).

Genomic Library Construction, 454 Genome Sequencing, and Annotation. The genomic library was constructed according to standard procedures.[74] Genomic DNA was partially digested with *Sau*3AI. About 30−50 kb DNA fragments were isolated and subsequently ligated into the cosmid pJTU2554 that had been previously subjected to linearization by *Hpa*I, dephosphorylated by fast alkaline phosphatase (FastAP), and digested with *Bam*HI. MaxPlax Lambda packaging extracts were used to perform the in vitro packaging according to the standard protocol. The resulting *E. coli* clones were picked randomly, transferred to 20 96-well microplates, and then, stored at −80 °C.

dx.doi.org/10.1021/ja3069243 | *J. Am. Chem. Soc.* 2013, 135, 1739−1748

The genomic DNA was isolated, and the ratio of A260/A280 was measured as 1.83.[75] After three rounds of 454 genome sequence, about 740 contiguous fragments that covered a total length of 7.1 Mb DNA sequences were obtained. Sequences of contiguous fragments were analyzed. We identified a fragment covering a 65.5 kb DNA region in which the gene *stnQ1* showed high homology to the reported methyltransferase MppJ involved in mannopeptimycin biosynthesis.[36] The PCR primers for genome screening and walking through the whole genomic library were designed, and three cosmids were confirmed to cover the 65.5kb DNA region.

The DNA sequence of the *stn* gene cluster has been deposited into GenBank under the accession number JQ414024. The analysis of orfs and the function predictions were carried out by Frame plot 4.0 beta (http://nocardia.nih.go.jp/fp4/), NCBI blast program (http://blast.ncbi.nlm.nih.gov/Blast.cgi), and Pfam 26.0 (http://pfam.janelia.org/). The *S. flocculus* CGMCC 4.1223 genome annotations were accomplished with Glimmer (http://cbcb.umd.edu/software/glimmer/).

Construction of Gene Inactivation Mutants. The PCR-targeting gene replacements were carried out according to the standard method.[76] Subclones were used with pJTU1289 to include the target genes in this study (Table S4, Supporting Information).[77] All the PCR-targeting vectors used in this study were constructed by a similar strategy (see the Supporting Information). The construction strategy of large fragment deletion mutant differs from that of the PCR-targeting gene replacement; detailed construction strategies of all the mutants were summarized in the Supporting Information. The resulting gene inactivation vectors were then transformed into *E. coli* ET12567/pUZ8002, and the conjugations were performed using the spores of *S. flocculus* CGMCC 4.1223 that were treated according to standard methods.[75] Double-crossover mutants were identified through diagnostic PCR with corresponding primers (Table S5, Supporting Information).

Fermentation and HPLC Analyses of All Strains. Wild-type and all mutant strains were fermented in the same culture condition. The strains were first cultured in seed medium TSBY (3% TSB and 0.5% yeast extract) for 2−3 days, and then, 1% inoculums were cultured in producing medium (2.5% glucose, 1.5% soybean, 0.5% NaCl, 0.05% KCl, 0.025% $MgSO_4 \cdot 7H_2O$, 0.3% K_2HPO_4, and 0.3% $Na_2HPO_4 \cdot 12H_2O$) for 7−8 days.[78] After finishing the fermentation, the broths were harvested by centrifugation and extracted with ethyl acetate. The resultant organic phase was concentrated and analyzed by HPLC or LC-MS that was carried out using a reverse-phase column ZORBAX SB-C18 (Agilent, 5 μm, 150 mm × 4.6 mm) with UV detection at 210, 245, and 375 nm under the following conditions: 10−70% B (linear gradient, 0−40 min; A, Milli-Q water; B, acetonitrile), 70−100 B% (linear gradient, 41−45 min), 100% B (45−50 min) at the flow rate of 0.6 mL min^{-1}.

General Materials and Instruments for Compound Purification and Characterization. Materials for column chromatography (CC) were silica gel (80−100 mesh; 200−300 mesh; 300−400 mesh. Haiyang Silica gel development Inc. Qingdao, China), reverse-phase silica gel (C18, 50 μm, YMC, Japan), and molecular sieve (Sephadex LH-20, GE, USA). The lyophilizer was Chaist alpha 1−2. HPLC was conducted on Agilent series 1200 and 1260 with the reverse-phase column ZORBAX SB-C18 (5 μm, 4.6 mm × 150 mm) and the semipreparative column XDB-C18 (5 μm, 9.4 mm × 250 mm). The LC-MS analyses were performed on an Agilent series 1100 LC/MSD trap, and high-resolution MS analyses were carried out on a 6530 Accurate-Mass Q-TOF spectrometer coupled to an Agilent HPLC 1200 series (Agilent Technologies). ^1H, ^{13}C, and 2D NMR spectra were recorded on a Bruker AV-500 MHz NMR spectrometer with tetramethylsilane (TMS, 0.0 ppm) as the internal standard. All the analogue isolation procedures and the feeding experiments were described in the Supporting Information.

Cloning, Expression, Purification, and in Vitro Assay of StnB1/B2. The *stnB1* and *stnB2* genes were amplified from cosmid p4D6 using high fidelity DNA polymerase KOD plus (TOYOBO). The primer pairs were listed in Table S5 of the Supporting Information. Both PCR products were digested with *Nde*I/*Xho*I and inserted into pET28a to give the expression plasmids (Table S4, Supporting Information). After sequence confirmation, the constructed clones pJTU4027 and pJTU4028 were transformed into *E.coli* BL21 (DE3). After the cells harboring the desired plasmids were grown in LB medium at 37 °C to an A_{600} of about 0.6 and induced by the addition of 0.8 mM isopropyl-β-D-thiogalactopyranoside (IPTG), the cells were incubated at 16 °C for an additional 20 h. Cells were harvested by centrifugation (8000 rpm for 5 min at 4 °C) and resuspended in buffer A (20 mM Tris−HCl, 500 mM NaCl, 40 mM imidazole, 10% glycerol, pH 7.5). Purification of the N-terminal His_6-tagged fusion protein with Ni−NTA affinity resin was performed according to manufacturer's protocols, using a HisTrapTM HP column (1 mL) on the fast protein liquid chromatograph (FPLC). After purification, StnB1 was reconstituted using the following procedures: 5 mM DTT was added first. After 15 min, 1 mM $Fe(NH_4)_2(SO_4)_2$ was added, and 1 mM Na_2S was then added with 15 min interval; the resulting mixture was incubated for another 45 min. After finishing the reconstitution, the protein was purified and desalted. The yield of the overproduced StnB2 was much higher than that of StnB1, so after purification, we diluted the StnB2 proteins to the same concentration with that of StnB1, mixed together and packaged into small portions to simplify the experimental operation. Finally, these two proteins were analyzed by sodium dodecyl sulfate polyacrylamide gel electrophoresis (SDS-PAGE) to check purity and stored at −80 °C in storage buffer (50 mM Tris−HCl, pH 7.9, 50 mM NaCl, 5% glycerol). The in vitro assay condition was in a 500 μL reaction: 50 mM MES buffer (pH 6.8), 0.1 mM ammonium ferrous sulfate, 50 mM NaCl, 1 mM sodium dithionite, 2 μM StnB1/B2 mixtures, and 100 μM compound **7** or **8** dissolved in DMSO (final concentration was 5% DMSO solution).[79−81] The reaction was performed at 30 °C and incubated for 4 h. Then, the reaction was quenched using 500 μL of ethyl acetate for extraction twice. After removing ethyl acetate by vacuum evaporation, the residues were dissolved in 50 μL of methanol and subjected to LC-MS analysis. The cosubstrates reaction was performed with adding 100 μM compounds **7** and **8** together in one 500 μL reaction. The reaction solution was analyzed by HR-MS when incubated for 15 min, 30 min, 1 h, 1.5 h, and 2 h, and each time about 100 μL of the solution was taken for HR-MS analysis.

Cloning, Expression, Purification, and in Vitro Assay of StnF1/F2. The *stnF1* and *stnF2* genes were amplified from cosmid p4D6 and p4F4, respectively, using high fidelity DNA polymerase KOD plus (TOYOBO). The primers were listed in Table S5 of the Supporting Information. PCR products were then digested with *Nde*I/*Xho*I and inserted into pET28a treated by *Nde*I/*Xho*I to give the expression plasmids (Table S4, Supporting Information). After sequence confirmation, the constructed plasmids pJTU4037 and pJTU4038 were transformed into *E.coli* BL21 (DE3) for protein expression. The cells harboring the desired plasmids were grown in LB medium at 37 °C to an A_{600} of about 0.6, induced by the addition of 0.4 mM IPTG, and then, incubated at 16 °C for an additional 20 h. Cells were harvested by centrifugation (8000 rpm for 5 min at 4 °C) and resuspended in buffer A (20 mM Tris−HCl, 500 mM NaCl, 40 mM imidazole, 10% glycerol, pH 7.5). Purification of the N-terminal His_6-tagged fusion protein with Ni−NTA affinity resin was performed according to the manufacturer's protocols, using a HisTrapTM HP column (1 mL) on the FPLC. The in vitro assay condition in a 100 μL reaction was listed as follows: 50 mM Tris−HCl buffer (pH 8.0), 5 mM $MgCl_2$, 2 mM SAM, 0.5 mM substrate **7** in DMSO (final concentration), and 10 μM StnF1 or StnF2. After the reaction solutions were incubated at 30 °C for 2 h,[36,67] the reactions were quenched using 200 μL of ethyl acetate for extraction twice. After removing ethyl acetate by vacuum evaporation, the residues were dissolved in 20 μL of methanol and subjected to LC-MS analysis. The controls were carried out in the same condition with the boiled enzymes.

■ ASSOCIATED CONTENT

Supporting Information

Some results and experimental procedures; bacterial strains, plasmids, primers, and compound characterization including MS spectra and NMR data and spectra; HPLC and UV absorption profiles; construction and genotype analysis of gene inactivation mutants, construction of gene expression plasmids, and SDS-PAGE of proteins. This material is available free of charge via the Internet at http://pubs.acs.org.

■ AUTHOR INFORMATION

Corresponding Author

linsj@sjtu.edu.cn

Notes

The authors declare no competing financial interest.

■ ACKNOWLEDGMENTS

This work was financially supported by the 973 and 863 programs from MOST, the key project (311018) and New Century Training Program Foundation for the Talents from MOE, and the National Natural Science Foundation of China (NNSFC).

■ REFERENCES

(1) Rao, K. V.; Cullen, W. P. *Antibiot. Annu.* **1959**, *7*, 950.
(2) Rao, K. V.; Biemann, K.; Woodward, R. B. *J. Am. Chem. Soc.* **1963**, *85*, 2532.
(3) Chiu, Y. Y. H.; Lipscomb, W. N. *J. Am. Chem. Soc.* **1975**, *97*, 2525.
(4) Lown, J. W.; Begleiter, A. *Can. J. Chem.* **1974**, *52*, 2331.
(5) Oleson, J. J.; Calderella, L. A.; Mjos, K. J.; Reith, A. R.; Thie, R. S.; Toplin, I. *Antibiot. Chemother.* **1961**, *11*, 158.
(6) Reilly, H. C.; Sugiura, K. *Antibiot. Chemother.* **1961**, *11*, 174.
(7) Beall, H. D.; Mulcahy, R. T.; Siegel, D.; Traver, R. D.; Gibson, N. W.; Ross, D. *Cancer Res.* **1994**, *54*, 3196.
(8) Beall, H. D.; Murphy, A. M.; Siegel, D.; Hargreaves, R. H.; Butler, J.; Ross, D. *Mol. Pharmacol.* **1995**, *48*, 499.
(9) Humphrey, E. W.; Blank, N. *Cancer Chemother. Rep.* **1961**, *12*, 99.
(10) Harris, M. N.; Medrek, T. J.; Golomb, F. M.; Gumport, S. L.; Postel, A. H.; Wright, J. C. *Cancer* **1965**, *18*, 49.
(11) Hackethal, C. A.; Golbey, R. B.; Tan, C. T.; Karnofsky, D. A.; Burchenal, J. H. *Antibiot. Chemother.* **1961**, *11*, 178.
(12) Hajdu, J.; Armstrong, E. C. *J. Am. Chem. Soc.* **1981**, *103*, 232.
(13) White, J. R. *Biochem. Biophys. Res. Commun.* **1977**, *77*, 387.
(14) Rao, K. V. *J. Pharm. Sci.* **1979**, *68*, 853.
(15) Sugiura, Y.; Kuwahara, J.; Suzuki, T. *Biochim. Biophys. Acta, Gene Struct. Expression* **1984**, *782*, 254.
(16) Donohoe, T. J.; Jones, C. R.; Barbosa, L. C. A. *J. Am. Chem. Soc.* **2011**, *133*, 16418.
(17) Bringmann, G.; Reichert, Y.; Kane, V. V. *Tetrahedron* **2004**, *60*, 3539.
(18) Boger, D. L.; Panek, J. S.; Duff, S. R. *J. Am. Chem. Soc.* **1985**, *107*, 5745.
(19) Kende, A. S.; Lorah, D. P.; Boatman, R. J. *J. Am. Chem. Soc.* **1981**, *103*, 1271.
(20) Basha, F. Z.; Hibino, S.; Kim, D.; Pye, W. E.; Wu, T. T.; Weinreb, S. M. *J. Am. Chem. Soc.* **1980**, *102*, 3962.
(21) Weinreb, S. M.; Basha, F. Z.; Hibino, S.; Khatri, N. A.; Kim, D.; Pye, W. E.; Wu, T. T. *J. Am. Chem. Soc.* **1982**, *104*, 536.
(22) Shaikh, I. A.; Johnson, F.; Grollman, A. P. *J. Med. Chem.* **1986**, *29*, 1329.
(23) Gerwick, W. J.; Gould, S. J.; Fonouni, H. *Tetrahedron Lett.* **1983**, *24*, 5445.
(24) Gould, S. J.; Cane, D. E. *J. Am. Chem. Soc.* **1982**, *104*, 343.
(25) Gould, S. J.; Erickson, W. R. *J. Antibiot.* **1988**, *41*, 688.
(26) Gould, S. J.; Chang, C. C. *J. Am. Chem. Soc.* **1977**, *99*, 5496.
(27) Gould, S. J.; Chang, C. C. *J. Am. Chem. Soc.* **1978**, *100*, 1624.
(28) Gould, S. J.; Darling, D. S. *Tetrahedron Lett.* **1978**, *19*, 3207.
(29) Gould, S. J.; Chang, C. C. *J. Am. Chem. Soc.* **1980**, *102*, 1702.
(30) Gould, S. J.; Chang, C. C.; Darling, D. S.; Roberts, J. D.; Squillacote, M. *J. Am. Chem. Soc.* **1980**, *102*, 1707.
(31) Erickson, W. R.; Gould, S. J. *J. Am. Chem. Soc.* **1985**, *107*, 5831.
(32) Erickson, W. R.; Gould, S. J. *J. Am. Chem. Soc.* **1987**, *109*, 620.
(33) Hartley, D. L.; Speedie, M. K. *Biochem. J.* **1984**, *220*, 309.
(34) Doyle, T. W.; Balitz, D. M.; Grulich, R. E.; Nettleton, D. E.; Gould, S. J.; Tann, C.; Moews, A. E. *Tetrahedron Lett.* **1981**, *22*, 4595.
(35) Herlt, A. J.; Rickards, R. W.; Wu, J. P. *J. Antibiot.* **1985**, *38*, 516.
(36) Huang, Y. T.; Lyu, S. Y.; Chuang, P. H.; Hsu, N. S.; Li, Y. S.; Chan, H. C.; Huang, C. J.; Liu, Y. C.; Wu, C. J.; Yang, W. B. *ChemBioChem* **2009**, *10*, 2480.
(37) Li, L.; Xu, Z.; Xu, X.; Wu, J.; Zhang, Y.; He, X.; Zabriskie, T. M.; Deng, Z. *ChemBioChem* **2008**, *9*, 1286.
(38) Law, C. J.; Maloney, P. C.; Wang, D. N. *Annu. Rev. Microbiol.* **2008**, *62*, 289.
(39) Liu, W. C.; Barbacid, M.; Bulgar, M.; Clark, J. M.; Crosswell, A. R; Dean, L.; Doyle, T. W.; Fernandes, P. B.; Huang, S.; Manne, V. *J. Antibiot.* **1992**, *45*, 454.
(40) Pollegioni, L.; Molla, G.; Sacchi, S.; Rosini, E.; Verga, R.; Pilone, M. S. *Appl. Microbiol. Biotechnol.* **2008**, *78*, 1.
(41) Pollegioni, L.; Piubelli, L.; Sacchi, S.; Pilone, M. S.; Molla, G. *Cell. Mol. Life Sci.* **2007**, *64*, 1373.
(42) Vaillancourt, F. H.; Yeh, E.; Vosburg, D. A.; O'Connor, S. E.; Walsh, C. T. *Nature* **2005**, *436*, 1191.
(43) Neumann, C. S.; Walsh, C. T. *J. Am. Chem. Soc.* **2008**, *130*, 14022.
(44) Khare, D.; Wang, B.; Gu, L.; Razelun, J.; Sherman, D. H.; Gerwick, W. H.; Hakansson, K.; Smith, J. L. *Proc. Natl. Acad. Sci. U.S.A.* **2010**, *107*, 14099.
(45) Koketsu, K.; Watanabe, K.; Suda, H.; Oguri, H.; Oikawa, H. *Nat. Chem. Biol.* **2010**, *6*, 408.
(46) Xu, Y.; Kersten, R. D.; Nam, S. J.; Lu, L.; Al-Suwailem, A. M.; Zheng, H. J.; Fenical, W.; Dorrestein, P. C.; Moore, B. S.; Qian, P. Y. *J. Am. Chem. Soc.* **2012**, *134*, 8625.
(47) Reimer, D.; Pos, K. M.; Thines, M.; Grün, P.; Bode, H. B. *Nat. Chem. Biol.* **2011**, *7*, 888.
(48) Zhu, Y.; Fu, P.; Lin, Q.; Zhang, G.; Zhang, H.; Li, S.; Ju, J.; Zhu, W.; Zhang, C. *Org. Lett.* **2012**, *14*, 2666.
(49) Funabashi, M.; Yang, Z.; Nonaka, K.; Hosobuchi, M.; Fujita, Y.; Shibata, T.; Chi, X.; Van Lanen, S. G. *Nat. Chem. Biol.* **2010**, *6*, 581.
(50) Liao, R.; Liu, W. *J. Am. Chem. Soc.* **2011**, *133*, 2852.
(51) Lin, S.; Hanson, R. E.; Cronan, J. E. *Nat. Chem. Biol.* **2010**, *6*, 682.
(52) Carr, P. D.; Ollis, D. L. *Protein Pept. Lett.* **2009**, *16*, 1137.
(53) Butler, C. S.; Mason, J. R. *Adv. Microb. Physiol.* **1996**, *38*, 47.
(54) Heider, J.; Fuchs, G. *Eur. J. Biochem.* **1997**, *243*, 577.
(55) Abe, N.; Enoki, N.; Nakakita, Y.; Uchida, H.; Nakamura, T.; Munekata, M. *J. Antibiot.* **1993**, *46*, 1678.
(56) Nissen, F.; Detert, H. *Eur. J. Org. Chem.* **2011**, *2011*, 2845.
(57) Mizuno, N. *Biochem. Pharmacol.* **1967**, *16*, 933.
(58) Kremer, W. B.; Laszlo, J. *Biochem. Pharmacol.* **1966**, *15*, 1111.
(59) Nojiri, H.; Omori, T. *Biosci., Biotechnol., Biochem.* **2002**, *66*, 2001.
(60) Kumar, P.; Mohammadi, M.; Dhindwal, S.; Pham, T. T. M.; Bolin, J. T.; Sylvestre, M. *Biochem. Biophys. Res. Commun.* **2012**, *421*, 757.
(61) Tolstykh, T.; Lee, J.; Vafai, S.; Stock, J. B. *EMBO J.* **2000**, *19*, 5682.
(62) Lee, J. A.; Pallas, D. C. *J. Biol. Chem.* **2007**, *282*, 30974.
(63) Dhar, K.; Rosazza, J. P. N. *Appl. Environ. Microbiol.* **2000**, *66*, 4877.
(64) Ding, W.; Deng, W.; Tang, M.; Zhang, Q.; Tang, G.; Bi, Y.; Liu, W. *Mol. BioSyst.* **2010**, *6*, 1071.
(65) Zhao, Q.; He, Q.; Ding, W.; Tang, M.; Kang, Q.; Yu, Y.; Deng, W.; Zhang, Q.; Fang, J.; Tang, G. *Chem. Biol.* **2008**, *15*, 693.

(66) Isshiki, K.; Sawa, T.; Miura, K.; Li, B.; Naganawa, H.; Hamada, M.; Takeuchi, T.; Umezawa, H. *J. Antibiot.* **1986**, *39*, 1013.
(67) Kim, H. J; White-Phillip, J. A; Ogasawara, Y.; Shin, N.; Isiorho, E. A.; Liu, H. W. *J. Am. Chem. Soc.* **2010**, *132*, 2901.
(68) Walsh, C. T.; Haynes, S. W.; Ames, B. D. *Nat. Prod. Rep.* **2011**, *29*, 37.
(69) Knaggs, A. R. *Nat. Prod. Rep.* **2003**, *20*, 119.
(70) Laursen, J. B.; Nielsen, J. *Chem. Rev.* **2004**, *104*, 1663.
(71) Van Lanen, S. G.; Lin, S.; Shen, B. *Proc. Natl. Acad. Sci. U.S.A.* **2008**, *105*, 494.
(72) Sundlov, J. A.; Garringer, J. A.; Carney, J. M.; Reger, A. S.; Drake, E. J.; Duax, W. L.; Gulick, A. M. *Acta Crystallogr., Sect. D.: Biol. Crystallogr.* **2006**, *62*, 734.
(73) Khalil, S.; Pawelek, P. D. *Biochemistry (Moscow)* **2011**, *50*, 533.
(74) Sambrook, J.; Russell, D. W. *Molecular Cloning: a Laboratory Manual*; Cold Spring Harbor Laboratory Press: Woodbury, NY, 2001; Vol. 2.
(75) Kieser, T.; Bibb, M. J.; Buttner, M. J.; Chater, K. F.; Hopwood, D. A. *Practical Streptomyces Genetics*; The John Innes Foundation: Norwich, U.K., 2000.
(76) Gust, B.; Kieser, T.; Chater, K. *PCR Targeting System in Streptomyces coelicolor A3(2)*; The John Innes Foundation: Norwich, U.K., 2002.
(77) He, Y.; Wang, Z.; Bai, L.; Liang, J.; Zhou, X.; Deng, Z. *J. Microbiol. Biotechnol.* **2010**, *20*, 678.
(78) Smanski, M. J.; Yu, Z.; Casper, J.; Lin, S.; Peterson, R. M.; Chen, Y.; Wendt-Pienkowski, E.; Rajski, S. R.; Shen, B. *Proc. Natl. Acad. Sci. U.S.A.* **2011**, *108*, 13498.
(79) Hurtubise, Y.; Barriault, D.; Powlowski, J.; Sylvestre, M. *J. Bacteriol.* **1995**, *177*, 6610.
(80) Hurtubise, Y.; Barriault, D.; Sylvestre, M. *J. Biol. Chem.* **1996**, *271*, 8152.
(81) Wolfe, M. D.; Parales, J. V.; Gibson, D. T.; Lipscomb, J. D. *J. Biol. Chem.* **2001**, *276*, 1945.